Theor Chim Acta (1986) 69: 309-322

Theoretica Chimica Acta

Reaction dynamics on bifurcating potential energy surfaces

Wayne A. Kraus and Andrew E. DePristo*

Department of Chemistry, Iowa State University, Ames, IA 50011, USA

Received October 15, revised and accepted December 12, 1985)

Classical trajectories were run on a local fit to the bifurcating transition region of the Valtazanos and Ruedenberg *ab initio* potential energy surface for the cyclopropylidene to allene reaction, and also on several variations of this local surface. The trajectory results were analyzed to determine the outcome as a function of initial conditions, and several plots of these are presented.

Key words: Bifurcation transition region — Dynamic behavior — Trajectory analysis

1. Introduction

Recently, a potential energy surface exhibiting a bifurcating transition *region* has been found in the Valtazanos and Ruedenberg *ab initio* calculations for the ring opening reaction of cyclopropylidene to allene [1]. A bifurcating region, which has been considered in the literature [2-6], is not the same as the accidental occurrence of a bifurcating transition *state* [7]. The finding of this *ab initio* surface has prompted us to undertake the present study of the characteristic dynamic behavior expected on these types of surfaces. The calculations were done using classical trajectory analysis [8], as detailed in Sect. 2, and the results are presented in Sect. 3.

2. Calculations

The possible arrangements, denoted by *A*, *B*, and *C* for the cyclopropylidene-allene reaction, are defined in Fig. 1. Notice that the two forms of allene, while differing only in the 180° difference in orientation of one of the CH_2 groups

* Camille and Henry Dreyfus Teacher-Scholar; Alfred P. Sloan Foundation fellow

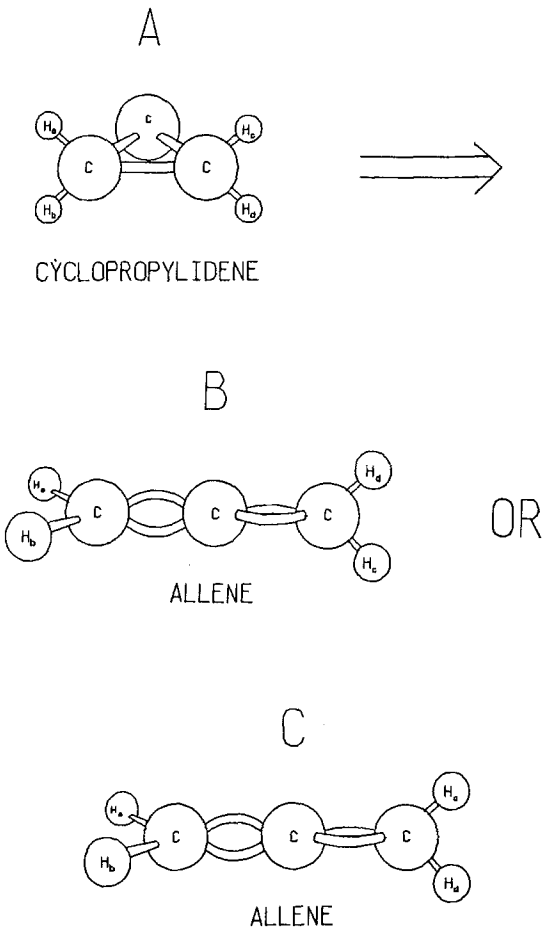

Fig. 1. Labeling of the 3 different forms of C_3H_4 in this study

relative to the other and therefore being quantum mechanically indistinguishable, can indeed be distinguished in a classical analysis. The surfaces (Figs. 2–5) are all obtained from the Valtazanos and Ruedenberg *ab initio* surface (Figs. 12 and 13 in [1]), by a local fit in the case of Surface 1 (Fig. 2), and by varying the surface parameters for Surfaces 3 and 4 (Figs. 4–5). For the second surface, we have modified Surface 1 by the addition of a small gaussian centered on the left saddle point to break the symmetry of these surfaces (Fig. 3). This case would then involve a bifurcation to products which are indeed distinguishable, although the surface is purely formal and does not correspond to a known physical reaction.

Valtazanos and Ruedenberg calculated their *ab initio* surface using MCSCF theory, and optimizing all but two coordinates, denoted by x and y, defined below. They fit their surface in the transition region with the following local power series expansion:

$$V = Ax - B(x + C_1 y^2)(x + C_2 y^2) \tag{1}$$

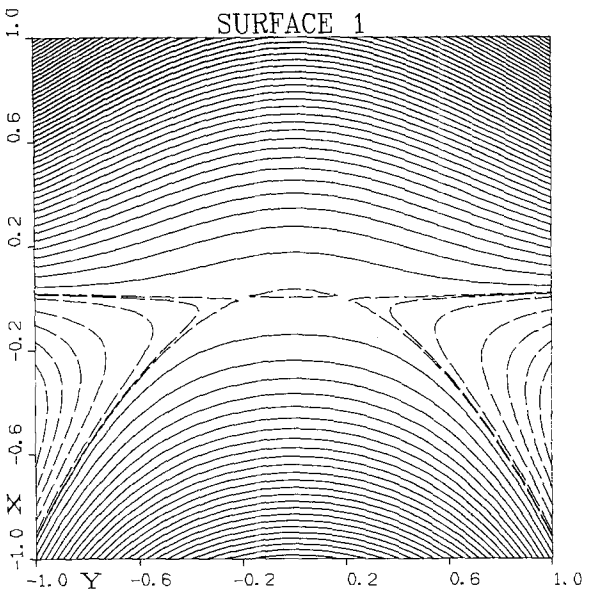

Fig. 2. The local fit to the Valtazanos and Ruedenberg surface [1]. *Dashed lines* represent equipotentials lying above the saddle point energy and *solid lines* those lying below it. The *dashed equipotential lines* are at 0.005 H, 0.01 H, 0.02 H and every 0.05 H thereafter, while the *solid lines* are at −0.03 H and every −0.05 H thereafter

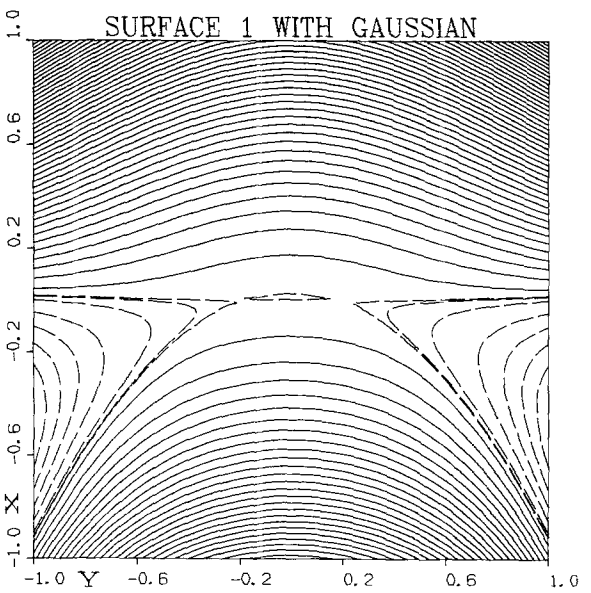

Fig. 3. *Dashed lines* represent equipotentials lying above the right saddle point energy and *solid lines* those lying below it. Contour intervals are the same as in Fig. 2

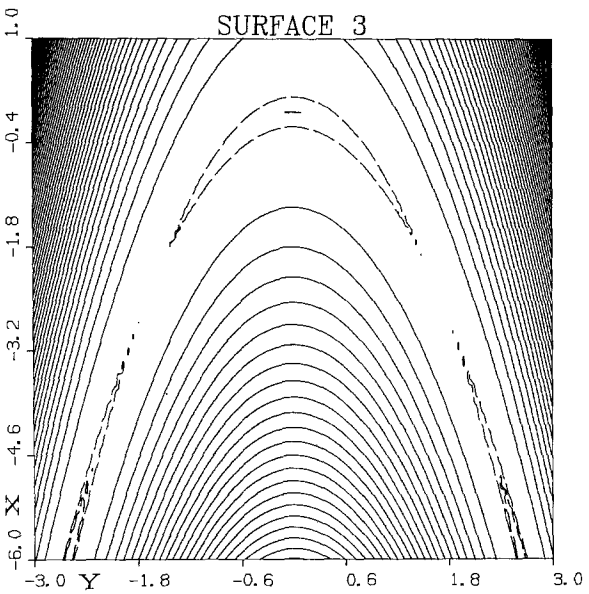

Fig. 4. *Dashed lines* represent equipotentials lying above the saddle point energy and *solid lines* those lying below it. The *dashed equipotential line* is at −0.05 H while the *solid lines* are at −2.0 H and every −2.0 H thereafter

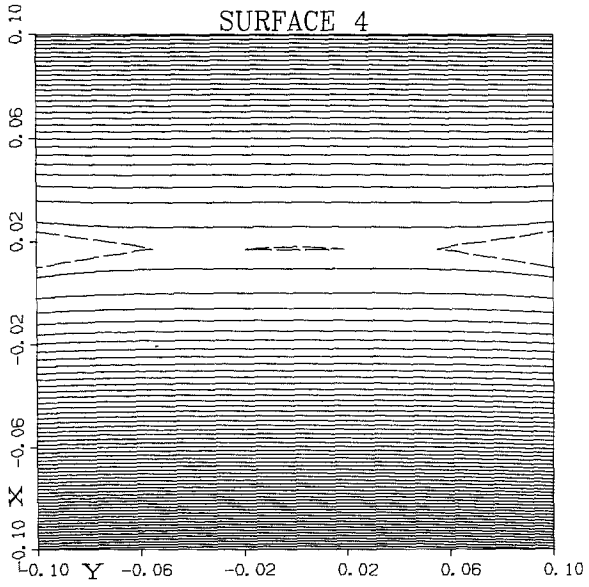

Fig. 5. *Dashed lines* represent equipotentials lying above the saddle point energy and *solid lines* those lying below it. The *dashed equipotential lines* are at 0.000383 H, while the *solid lines* are at 0.0003 H, 0.0 H and every −0.0003 H thereafter

where (i) x is the C-C-C angle, ranging from about 1.05 radians (60°) for cyclopropylidene to π radians for allene; (ii) y is one half the difference between the dihedral angles the CH_2 groups make with the plane of the three carbon atoms, ranging from 0 radians for cyclopropylidene to $\pi/4$ radians for allene; (iii) The surface is normalized such that $V=0$ at the valley ridge inflection Point, VRI, defined to be the point at which both x and y components of the gradient vanish; (iv) The coordinates are displaced so that the VRI point occurs at (0, 0).

This expansion, which corresponds to the cyclopropylidene-allene transition region for the specific set of parameters A, B, C_1, C_2 given in Table 1, will in fact represent such a bifurcating potential energy surface for any set of parameters such that

$$B>0, \qquad C_1+C_2>0. \tag{2}$$

These characteristics assure that a cross section of the surface in the x direction for values of $x<0$ (below the VRI point) will be a "valley" about the x axis, while such a cross section for $x>0$ will be a "ridge".

The surface defined by a given set of parameters can be further characterized in terms of its critical points. For $A\leq 0$ there is one critical point at $(A/2B, 0)$, with

$$V=\frac{A^2}{4B}$$

When $A<0$ this is a saddle point which occurs ahead of (below) the VRI point. If $A=0$ this is a higher order critical point which coincides with the VRI point. Dynamics on such surfaces are not investigated here since they do not exhibit a bifurcating transition region in the entrance channel.

If $A>0$ however, there are three critical points on the surface, a local maximum on the x axis at $(A/2B, 0)$ where

$$V=\frac{A^2}{4B}$$

and two saddle points located symmetrically about the x axis at

$$\left(\frac{-2AC_1C_2}{B(C_1-C_2)^2}, \frac{\pm\sqrt{A(C_1+C_2)/B}}{(C_1-C_2)}\right)$$

Table 1. Surface expansion parameters[a]

Surface	Fig.	A (H/radian)	B (H/radian^2)	C_1 (radian^{-1})	C_2 (radian^{-1})
1	2	0.04330895	1.21976773	0.95098511	−0.01970982
3	4	0.04331	1.2198	0.9510	0.8
4	5	0.04331	1.2198	0.9510	−0.8

[a] The parameters are defined in Eq. (1). The energy unit is the Hartree, symbolized by H

where

$$V = \frac{-A^2 C_1 C_2}{B(C_1 - C_2)^2}.$$

All the surfaces in this paper are examples of this kind of surface. Indeed, the surfaces other than Surface 1 were arrived at by modifying the parameters so as to alter the topology, characterized by the relative positions and energies of its critical points, with the least possible alteration of the original energy relationships. For convenience the parameters used in the various surfaces are summarized in Table 1. The locations and energies of critical points are given in Table 2.

In addition, we have introduced an asymmetric surface (Fig. 3) which is a modification of Surface 1 by the addition of the gaussian

$$2A_g \exp\left[-a(x-x_0)^2 - b(y-y_0)^2\right]$$

Table 2). The parameters (a, b, A_g) have the values (2000 radian^{-2}, 3.562 radian^{-2}, 0.0004 H) chosen arbitrarily but such that the original Surface 1 was not distorted except in the left hand transition region.

Although both coordinates are angles, we found it convenient to regard them as dimensionless displacements in a cartesian kinetic energy expression,

$$T = \tfrac{1}{2} I_x \dot{x}^2 + \tfrac{1}{2} I_y \dot{y}^2$$

This is valid since the analysis requires a very small region of the surface over which the moments of inertia would be essentially constant. The motion in the x direction, the ring opening, is thus referred to formally as a translational motion. Correspondingly we refer to the motion in the y direction, the CH_2 twist, as being vibrational since the cross sectional well for $x < 0$ is quartic.

The initial conditions for each trajectory were selected according to energy criteria as displayed graphically in Fig. 6. We defined the translational potential energy arbitrarily as the value of the lowest point within the well for a given value of x (which always lies on the x axis). Then the difference between this translational potential energy and the actual potential energy was defined to be the vibrational potential energy. E_{th} was defined to be the energy difference between the translational potential (potential at the bottom of the well) of the initial value of x,

Table 2. Critical points

		Local maximum			Saddle point		
Surface	Fig.	x (radian)	y (radian)	Value (H)	x (radian)	y (radian)	Value (H)
1	2	0.017753	0.0	0.00038443	0.0014126	±0.18733	0.000030589
3	4	0.017753	0.0	0.00038444	−2.36944	±1.65126	−0.051310
4	5	0.017753	0.0	0.00038444	0.017621	±0.041817	0.00038158

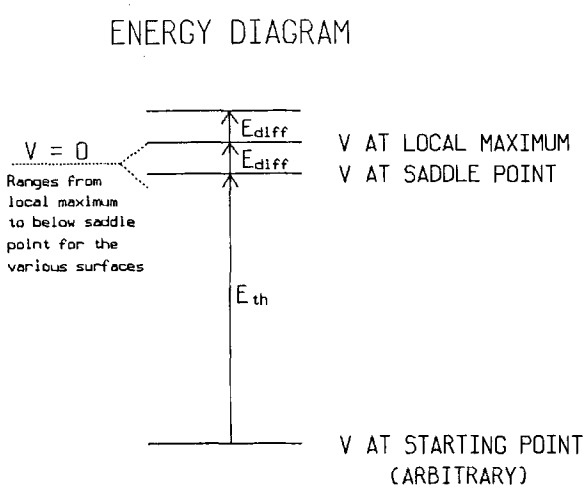

Fig. 6. Energy levels for the choice of translational and vibrational energies

chosen more or less arbitrarily, and the minimum energy for reaction to occur. For most of the surfaces vibrational energy had to be added for reaction to occur, since trajectories did not follow a minimum energy path. The trajectory results on each surface were analyzed both at this E_{th} and at another somewhat higher translational energy (within $2E_{\text{diff}}$ of E_{th}).

For each value of the translational energy, the vibrational energy and phase were scanned in the following way. The difference between the local maximum and the saddle point was defined to be E_{diff}, and the vibrational energy was varied from zero to twice E_{diff}. To scan the vibrational phase at each vibrational energy, we calculated the exact turning points from the potential energy surface at the specified initial value of x. This turning point was then taken as the amplitude of a sinusoidal oscillation of position. For each phase, given in degrees in the plots in Figs. 7–14, the corresponding position was computed which in turn yielded the vibrational potential energy, that is, the difference between the potential energy at that point and that of the bottom of the well. This value was subtracted from the specified vibrational energy and the result interpreted as vibrational kinetic energy, which provided the magnitude of the initial momentum in the y direction. The sign was derived from the assumed sinusoidal motion, guaranteeing that a 360° scan will sample the entire phase space. However, since the well was actually not quadratic but has a quartic term, this method of sampling did not quite distribute the trajectories evenly in phase space, but did guarantee that the entire phase space would be covered. The small anharmonicity would not significantly alter our results and at most would only slightly alter minor details of the appearance of our plots.

Thus each trajectory is specified by three parameters, translational energy, vibrational energy, and vibrational phase. The specified translational energy is converted directly into momentum in the positive x direction. For each value of the translational energy (two per surface) we scan vibrational energy from zero to

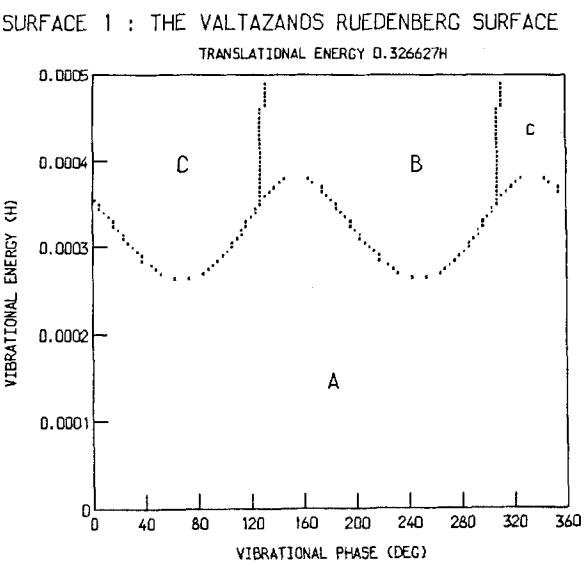

Fig. 7. Variation of reaction products with initial vibrational energy and phase

twice E_{diff}, and for each vibrational energy we scan the entire range of vibrational phase, 0–360°. We used moments of inertia of $I_x = m_C r_{CC}^2 = 153\,615 m_e$ bohr^2 and $I_y = 4 m_H r_{CH}^2 = 29\,826 m_e$ bohr^2 for the motions in the x and y coordinates, respectively. We emphasize that these are only estimates since the internal dynamics of the C_3H_4 molecule would need 18 dynamical degrees of freedom in an accurate treatment instead of 2.

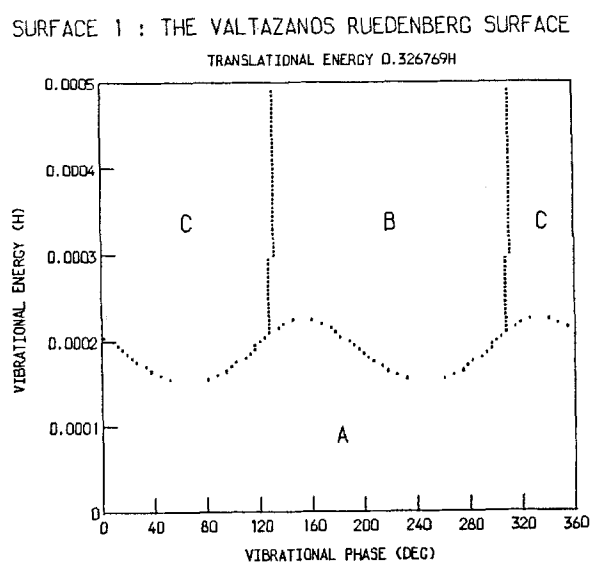

Fig. 8. Variation of reaction products with initial vibrational energy and phase

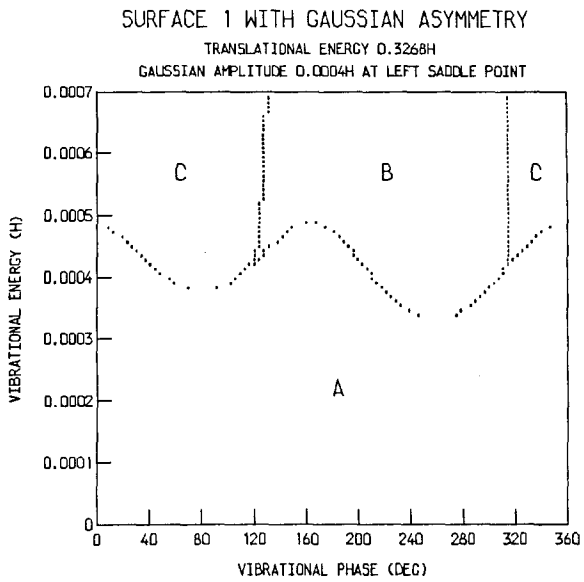

Fig. 9. Variation of reaction products with initial vibrational energy and phase

For each surface, one plot of results is provided for each of two values of the translational energy. Each plot covers the range of vibrational energies and vibrational phase. The plotted points represent boundaries between regions where the initial conditions lead to different products. The regions themselves are labeled according to the following convention (see also Fig. 1): *A* is cyclopropylidene,

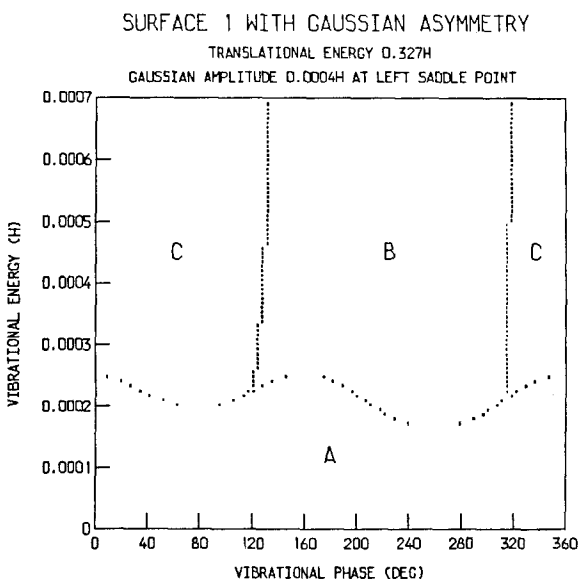

Fig. 10. Variation of reaction products with initial vibrational energy and phase

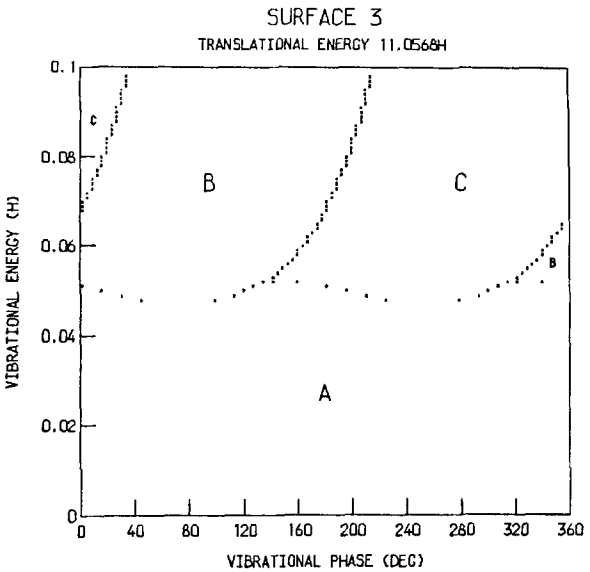

Fig. 11. Variation of reaction products with initial vibrational energy and phase

that is, no reaction occurred in these conditions; *B* is B allene (Fig. 1); *C* is C allene (Fig. 1). These plots were generated by scanning binary data files created by the integration program, and then edited for labels, titles, etc. using the UNIX system ged interactive graphics editor [9].

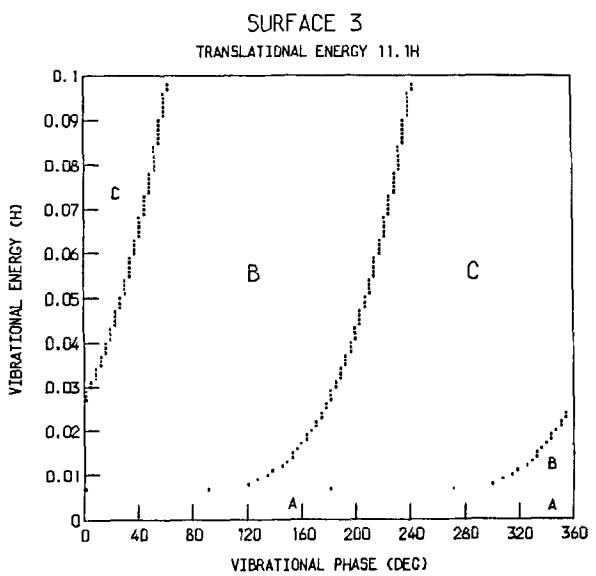

Fig. 12. Variation of reaction products with initial vibrational energy and phase

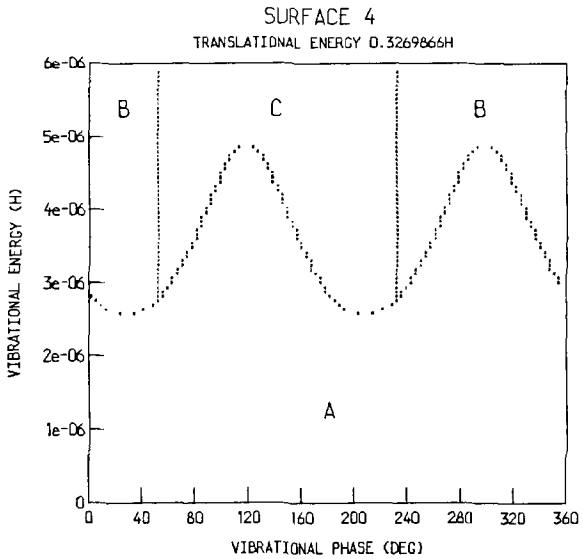

Fig. 13. Variation of reaction products with initial vibrational energy and phase

On Surface 1 (Fig. 2) translational energies of 0.326627 H (Fig. 7) and 0.326769 H (Fig. 8) were used. In these plots we note that first, no reaction occurs unless a certain amount of vibrational energy is present. This can be understood from the topography of the surface; if the energy is purely translational and does not exceed the local maximum on the x axis then no reaction can possibly occur. If, however, there is vibrational energy then the displacements in the y direction

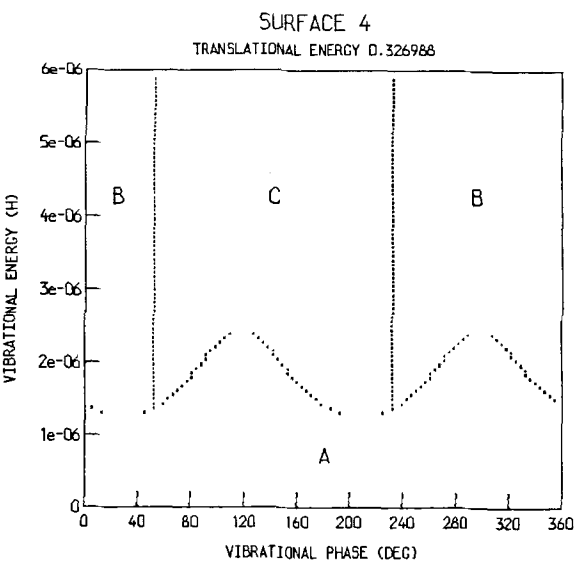

Fig. 14. Variation of reaction products with initial vibrational energy and phase

toward the saddle points would present lower barriers to reaction. Notice also that when sufficient vibrational energy is present, all trajectories lead to reaction. The products always occur in equal amounts, as they must by symmetry. The boundaries between B and C occur near the maxima of the sinusoid. This indicates that at lower energies the system necessarily passes through one saddle point or the other and subsequently is channeled into the corresponding product. This boundary does not occur exactly at the maximum, however, indicating that on this surface there is some crossover as the vibrational energy is increased, and the final result is no longer as definitely determined by which saddle point the system enters.

In comparing Figs. 7 and 8 we see that there is little structural difference with the latter displaced to lower vibrational energies and with lower amplitude to the sinusoidal reaction boundary. This indicates both that the reaction is enhanced by increasing the translational energy and that the vibrational energy then becomes less important. Presumably if the translational energy were increased still further a point would be reached where the dependence on vibrational energy would disappear.

On Surface 1 with a gaussian, Fig. 3 shows what happens when the symmetry is disturbed by adding a small gaussian distortion to the left saddle point (corresponding to C) of Surface 1 (Fig. 2). This surface was analyzed at translational energies of 0.3268 H (Fig. 9) and 0.327 H (Fig. 10). The most notable difference from the symmetric case is of course that the products no longer occur in equal amounts, but that C (corresponding to the saddle point with the gaussian) is inhibited relative to B. This is particularly true near the threshold, as expected, and begins to disappear as the energy (translational or vibrational) is increased, again demonstrating the decreasing importance of surface details in the transition region as energies are increased. Notice again that both vibrational and translational energies enhance the reaction in this case.

Surface 3 (Fig. 4) has the asymptotic curvature inflected downward in contrast to Surface 1. This surface was run at 11.0568 H (Fig. 11) and 11.1 H (Fig. 12). We notice at once that the boundary between B and C now rises almost exactly from the maximum of the sinusoid. This is to be expected, since it is clear from the surface that the connection between the saddle point the system passes through and the product state attained must be more direct. The saddle points of Surface 3, being more widely separated and with a larger local maximum between them, must exert a great deal of control over the final destination of the trajectories which pass through them. Again, in comparing these two plots, we find translational as well as vibrational enhancement.

Surface 4 (Fig. 5) has the same degree of curvature in the product channels as Surface 3, but with the same asymptotic direction of curvature as Surface 1 (Fig. 2). Notice that the scale of this plot is much smaller than the others. The channels are not nearly flat, as may appear, but comparable with those in Surface 3. The flat appearance arises from the fact that the saddle points have been compressed together into a very narrow region and now differ from the local maximum only

very slightly in energy. This surface was analyzed at 0.3269866 H (Fig. 13) and 0.326988 H (Fig. 14). The most notable difference is that the B-C boundary has moved nearly to the minimum of the sinusoid. This indicates that when conditions are suitable for the system to pass through one of the saddle points it is almost equally likely to go to either product. That is, the particular saddle point has much less control over the final result obtained. This must arise directly from the flatness of the surface about the transition region. In the transition region a trajectory is so close to the x axis that after passing through either saddle point it is still traveling along the ridge ($x > 0$) and can fall off into either product channel. Again both translational and vibrational enhancements are observed.

3. Conclusion

The main conclusion which arises from consideration of these results is that in general the behavior is in reasonable accord with expectations based upon consideration of the characteristics of the surfaces involved. The compactness of the product regions clearly indicates that chaos is not occurring. Indeed the simple two phase diagram present at high vibrational energy is especially regular. This is perhaps unexpected since the strong coupling of "translational" and "vibrational" motion might at least lead to a few distinct regions of different product formation.

All of the surfaces show a characteristic sinusoidal boundary between reactive and nonreactive regions. As discussed previously the amplitude of this sinusoid and its relation to the vertical boundary between the two product states correlate quite closely with the degree to which the particular saddle point the system passes through exerts control over which product state is finally attained. The results of the dynamical analysis on the gaussian modified surface indicate that even such a slightly asymmetrical surface would lead to preferential formation of one product over another under certain conditions. For example, at the lower translational energy in Fig. 9, at low vibrational energy only reactant A and product B appear. This point, applied to the question of reaction stereospecificity, was the original motivation of Valtazanos and Ruedenberg.

Finally it should be noted that we have referred to these surfaces as bifurcating surfaces since a quantum wavefunction would bifurcate on such a surface. In classical trajectory analysis, the totality of the trajectories sampling phase space models the actual bifurcation which would occur in such a quantum mechanical analysis. It might be an interesting problem to implement quantum dynamics, but it is not apparent that any different result could be expected, other than the obvious loss of some of the quantum mechanically undefined features we observed. Perhaps more interesting would be to incorporate all the internal degrees of freedom in the C_3H_4 system and analyze the dynamics on the full PES rather than a local fit to the transition region.

Acknowledgement. This work was partially supported by the National Science Foundation under grant CHE 8317882.

References

1. Ruedenberg K, Valtazanos P (1986) Theor Chim Acta 68:281–307
2. Goddard JD, Schaefer HF (1979) J Chem Phys 70:5117
3. Colwell SM (1984) Mol Phys 51:1217; Colwell SM, Handy NC (1985) J Chem Phys 82:1281
4. Tachibana A, Okazaki I, Koizumi M, Hori K, Yamabe T (1985) J Am Chem Soc 107:1190
5. Garrett BC, Truhlar DG, Wagner AF, Dunning TH (1983) J Chem Phys 78:4400
6. Miller WH (1983) J Phys Chem 87:21
7. Murrell JN, Laidler KJ (1968) Trans Far Soc 64:371; Murrell JN, Pratt GL (1970) Trans Far Soc 66:1680; Stanton RE, McIver JW (1975) J Am Chem Soc 97:3632; McIver JW (1974) Acc Chem Res 7:72
8. Porter RN, Raff LM (1976) In: Miller WH (ed) Dynamics of molecular collisions, part B, chapt 1. Plenum, New York
9. UNIX System V – Release 2.0, AT&T Bell Laboratories, 1984